THE STRUCTURE IN MESONIC CHANNELS ABOVE T_C

QCD-TARO COLLABORATION*

Quark-antiquark 4-point correlators in the mesonic channels at $T > 0$ are studied on the lattice to obtain insight into the hadronic and plasma physics of QCD.

Introduction We summarize results from comprehensive quenched SU(3) simulations for mesonic correlation functions[1,2,3]. From the propagation in Euclidean *time* (temperature) direction we extract *pole masses* and further structure of the *spectral functions*. By taking apart the quarks *spatially* we measure mesonic *wave functions*. The analysis involves various kinds of mesonic sources, fits of the spectral functions with pole and Breit-Wigner *ansätze*, extraction of the spectral function using MEM, and includes extensive tests. We recall that an Euclidean thermal propagator $G(t)$ is related by analytic continuation to the Minkowski propagator and hence to the spectral function $\rho(\omega)$ – see Fig. 1. Depending on T and on the operator used for meson the quantum state content and thus the spectral function ρ of the propagator varies. We can write down an integral equation for $\rho(\omega)$ using the simulation data for $G(t)$. This represents a typical "ill-posed problem" and needs "regularization" by physical (e.g., fit ansatz) or other kind of "a priori information" (e.g., Bayesian procedures).

We employ anisotropic lattices to have a finer t-discretization. We use Coulomb gauge and measure general 4-point functions:

$$G^{\Gamma}_{w}(r,t) = \sum_{\vec{R}} \sum_{\vec{s}_1,\vec{s}_2} w(\vec{s}_1,\vec{s}_2)\, \langle \gamma_5\, S(\vec{s}_1,0;\vec{r}_1,t)\, \gamma_5\, \Gamma_{\rm h}\, S(\vec{s}_2,0;\vec{r}_2,t)\, \Gamma_{\rm h} \rangle \quad (1)$$

with S : quark propagators, $\Gamma_{\rm h}$: γ_5 (ps.sc.), γ_i (vect.), 1 (sc.), $\gamma_5\,\gamma_i$ (ax. vect.). Summation over $\vec{R} = \frac{1}{2}(\vec{r}_1 + \vec{r}_2)$ is used to project total momentum 0, $\vec{r}_1 - \vec{r}_2 = \vec{r}$ enters the "wave function" $\phi(\vec{r};t)$ at t. $\vec{s}_1$, $\vec{s}_2$ are used to

*PH. DE FORCRAND (CERN and ETHZ, Switzerland), S. CHOE (KAIST, Daejon, Korea), M. GARCIA PEREZ (UAM, Madrid, Spain), Y. LIU (Nankai Univ., P. R. China), H. MATSUFURU (Kyoto Univ., Japan), O. MIYAMURA, A. NAKAMURA, K. NOMURA, T. TAKAISHI (Hiroshima Univ., Japan), I.-O. STAMATESCU (FEST and Heidelberg Univ., Germany), and T. UMEDA (Tsukuba Univ., Japan)

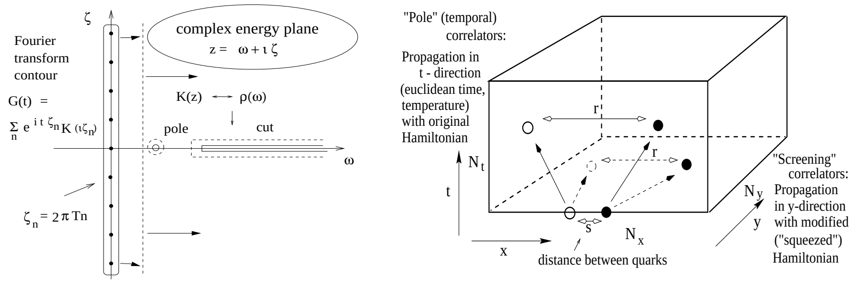

Figure 1. Complex energy plane with analytic continuation, and mesonic correlators. On the finite lattice the "cut" is made up of discrete contributions

construct initial states (sources). The smearing functions $w(\vec{x}_1, \vec{x}_2)$ are: $\delta(\vec{x}_1)\,\delta(\vec{x}_2)$ (point-point), $\delta(\vec{x}_1)\,\mathrm{e}^{-a\,|x_2|^p}$ (point-exp), $\mathrm{e}^{-a\,|x_1|^p}\,\mathrm{e}^{-a\,|x_2|^p}$ (exp-exp), and 1 (wall). The exp-exp (ee)-source is tuned slightly wider than the wave function of the meson at $T = 0$. We also compare with $G_0(t)$ obtained using free quark propagators S_0 in (1). We quote results from:
Simulation I[1]: Anisotropic lattice $12^3 \times N_\tau$, $a_\tau = a_\sigma/5.3 \simeq (4.5\mathrm{GeV})^{-1}$. Wilson Y-M, Wilson fermions, "light" quarks ($m_{ps} \sim 0.5$GeV) $N_\tau = 72,\ 20,\ 16,\ 12$ ($T \simeq$ "0", $0.93,\ 1.13,\ 1.5\ \times T_c$).
Simulation II[2]: Anisotropic lattice $16^2 \times 24 \times N_\tau$, $a_\tau = a_\sigma/3.95 \simeq (6.4\mathrm{GeV})^{-1}$. Symanzik improved Y-M, $O(a)$ improved Wilson fermions, "charm" quarks ($m_{ps} \sim 3$GeV). $N_\tau = 96,\ 26,\ 22,\ 16$ ($T \simeq$ "0", $0.93,\ 1.1,\ 1.52\ \times T_c$).
Simulation III[3]: Anisotropic lattice $20^3 \times N_\tau$, $a_\tau = a_\sigma/4 \simeq (8.1\mathrm{GeV})^{-1}$ Wilson Y-M, $O(a)$ improved Wilson fermions, "charm" quarks ($m_{ps} \sim$ 3GeV). $N_\tau = 160,\ 32,\ 26$ ($T \simeq$ "0", $0.88,\ 1.08\ \times T_c$).

Meson propagators and pole masses To extract the physical signal we use the "effective mass" $M(t)$ to parameterize $G(t) \simeq \cosh\left((N_\tau/2 - t)\,M(t)\right)$. At $T = 0$ $M(t)$ for the (ee) source is very flat, indicating that the propagator is dominated by a low energy pole at this mass (all sources agree at large t). With increasing T we see (Fig. 2):
For $T < T_c$ little difference to $T = 0$ for both light and charm mesons;
For $T > T_c$ increasing dependence of effective masses on t and source, and:
- *similarities* (t-dependence, hierarchy inversion) and *dissimilarities* (no common fit possible) compared with free quark propagation;
- chiral symmetry restoration above T_c for light mesons, together with linear mass increase with T for light and practically constant for charm mesons.

Meson wave function We calculate Coulomb gauge wave functions from correlators (1) with various initial states (sources) and $q\ \bar{q}$ in final

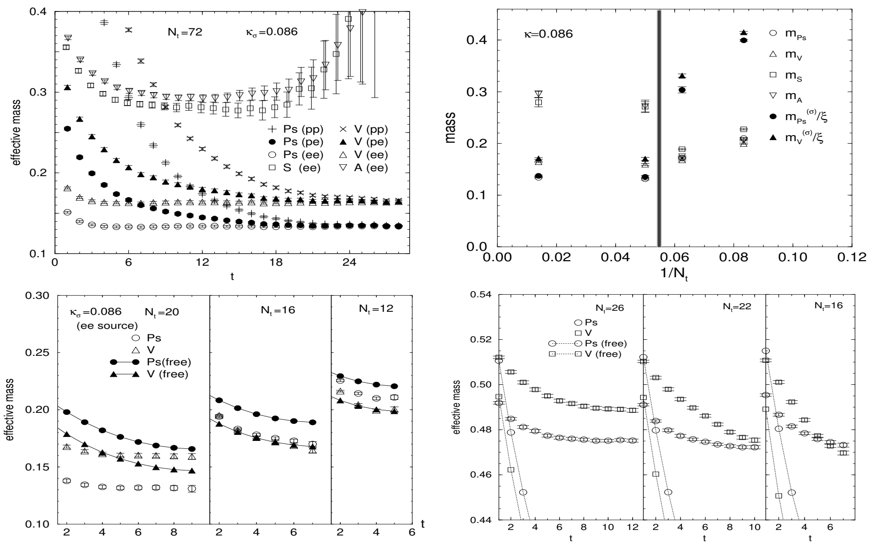

Figure 2. Effective masses $M(t)$: $T = 0$ from *Simulation I* (*upper left*), various mesons and sources; $T \simeq 0.93,\ 1.1$ and $1.5 \times T_c$ (from left to right) for "light" quarks (*Simulation I*, *lower left*) and "charm" (*Simulation II*, *lower right*) for *ps* and vector mesons with (*ee*) source. Also shown are the "free quark mesons". Notice the hierarchy inversion between pseudoscalar and vector at high temperature: this also indicates with T increasingly wide structure in the spectral function. *Upper right*: Lowest masses in the *ps*, *V*, *S* and *A* channels *vs* T (full symbols are "screening" masses). The vertical line is T_c.

state at spatial distance r: $\varphi(r,t) = G(r,t)/G(0,t)$. Again we compare with the $\varphi_0(r,t)$ from free quark propagators S_0 in $G(r,t)$. For a first trial we use the (*ee*) source (which was tuned slightly wider than the *measured* w.f. at $T = 0$). For bound quarks the shape of the w.f. should stabilize with increasing t, for unbound quarks it should become flatter. For a second trial we use various sources and measure the *average* r as function of t.
Both for "light" and charm quarks below **and** above T_c we see (Fig. 3):
- convergence with increasing t to well defined wave function $\simeq \exp(-ax^p)$ with typical mesonic parameters a, p, and stable $q - \bar{q}$ distance r,
- *source dependence* increasing with T,
- striking *difference* to unbound quarks at all T.

Thus *even at* $1.5\,T_c$ quarks appear *spatially correlated.* This suggests survival of mesonic excitations above T_c as *metastable* $q\,\bar{q}$ states.

Mesonic spectral function: Results from *Simulation III* Correlators (1) are measured for *ps* and vector mesons with point (*pp*) source and sink, and with smeared (*ee*) source and sink. Two methods are used to obtain

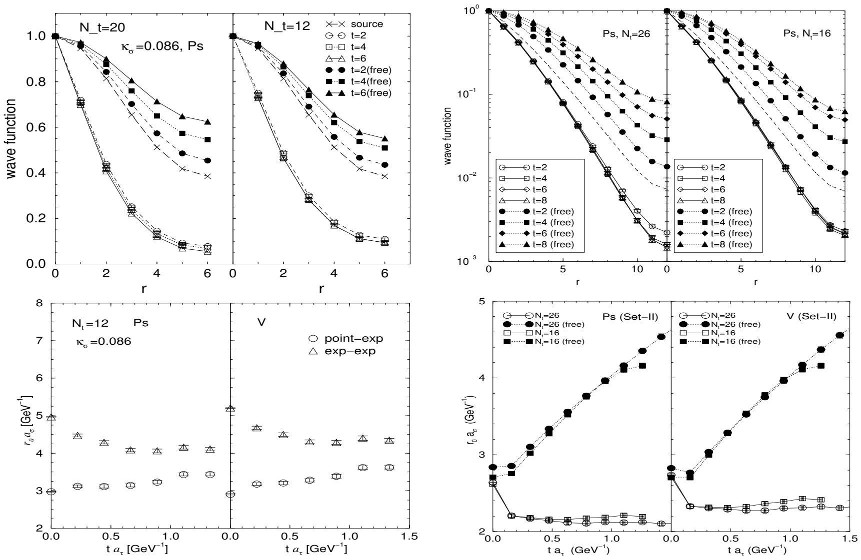

Figure 3. *Upper plots*: Pseudoscalar wave function $\varphi(r,t)$ at $T \simeq 0.93$ (left) and $1.5\,T_c$ (right) for light quarks at t = 2, 4 and 6 (*Simulation I*, (ee) source, *left plot*) and for charm at t = 2, 4, 6 and 8 (*Simulation II*, (ee) source, *right plot*). The free "wave function" $\varphi_0(r,t)$ (full symbols) flattens, as it should, while the meson wave function stabilizes rapidly. Expected below T_c (where we know that there is a bound state), *above T_c this is a non-trivial result! Lower plots*: Evolution of the average distance r_0 between $q-\bar{q}$ with t: *Simulation I* (*left plot*), pseudoscalar (left) and vector (right) for light quarks at $T = 1.5\,T_c$, various sources. A narrow initial distribution widens, a wide one narrows, tending toward a common limit; *Simulation II* (*Right plot*), (ee) source, the $q-\bar{q}$ distance stabilizes (while free quarks – full symbols – fly apart).

the solution of the integral equation:

$$G(t) = \int d\omega\, \rho(\omega)\, \frac{\cosh[\,\omega\,(N_\tau/2 - t)\,]}{2\sinh[\,\omega\, N_\tau/2\,]} \tag{2}$$

I. MEM: kernel inversion using singular value decomposition and maximal entropy method to constraint ρ in fitting the data.
II. Fit of the data with various ansätze for the spectral function: narrow states (poles) and wide states (modified Breit-Wigner).
In both cases tests are performed by varying the fit interval (t_{max}), number of data points etc. and also by checking the known results for free quarks. The summary of the analysis is (see Fig. 4 for some results):
- MEM for unsmeared source and $t_{max} < 24$ ($N_\tau < 48$) gives wrong results;
- for smeared operators and $t_{max} > 12$ (available for $N_\tau > 24 \sim 1.1\,T_c$; relevant parameter is the physical length $t_{max}a_\tau$): MEM gives reliable results for the lowest peak position, the width depends on default model; 1 BW

and BW + pole fits give consistent results for position *and* width. We find at $T \simeq 1.08\,T_c$: $Ps : m \sim 3.06, \gamma \sim 0.12$; $V : m \sim 3.13, \gamma \sim 0.21$ (GeV).

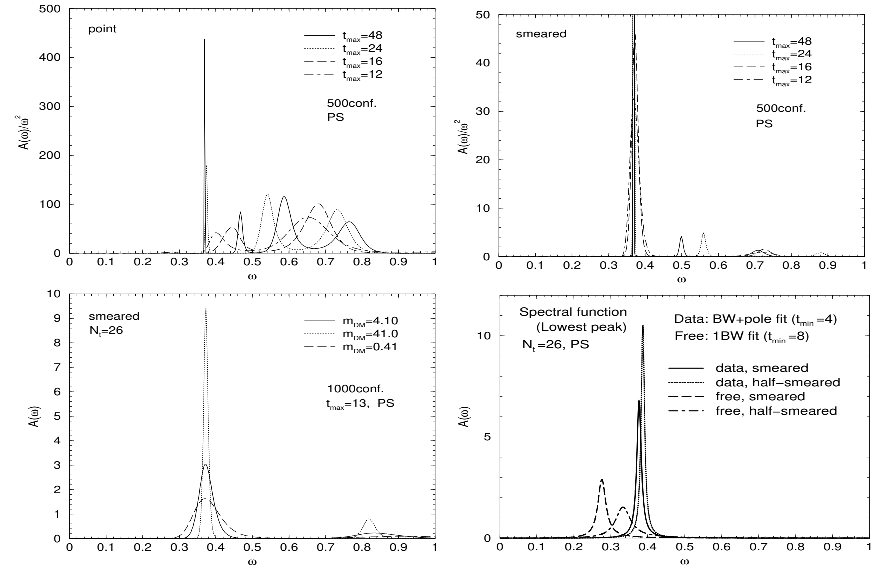

Figure 4. The *ps* $\rho(\omega)$. *Upper plots*: $T \simeq 0$, $20^3 \times 160$ lattice, **MEM** for point (*left plot*) and smeared operators (*right plot*) using the first t_{max} points in $G(t)$. *Lower plots*: $T \simeq 1.08\,T_c$, $20^3 \times 26$ lattice, **MEM** for smeared source, various "default model" parameters (*left plot*), and **Fit** with "BW + pole" and $\rho_0(\omega)$ with "BW" *ansatz*.

Conclusions Low energy, $q - \bar{q}$ excitations are seen in the mesonic channels up to $T \simeq 1.5T_c$, with stable spatial distribution $\simeq$ mesonic "wave function". We see chiral symmetry restoration at T_c. Thermal effects show up above T_c as increasing width and, for light mesons, increasing masses. The overall picture is that of quasistable states of quarks subject to thermal effects. Using smeared sources is useful for selecting meson-like states at small energy and appears justified by self-consistency. Direct extraction of the spectral function appears problematic for point-like sources at $T > 0$. Smeared sources allow consistent MEM and fit analyses up to at least $1.1T_c$.

References

1. QCD-TARO: Ph. de Forcrand et al.: *Phys. Rev.* **D63**, 054501 (2001).
2. T. Umeda et al.: *Int. J. Mod. Phys.* **A16**, 2215 (2001), hep-lat/0011085.
3. T. Umeda, K. Nomura and H. Matsufuru: "Charmonium at finite temperature in quenched lattice QCD", hep-lat/0211003.